antioxidants

Article

Tissue Distribution of Oleocanthal and Its Metabolites after Oral Ingestion in Rats

Anallely López-Yerena [1], Anna Vallverdú-Queralt [1,2], Olga Jáuregui [3], Xavier Garcia-Sala [4], Rosa M. Lamuela-Raventós [1,2] and Elvira Escribano-Ferrer [2,4,5,*]

1 Department of Nutrition, Food Science and Gastronomy XaRTA, Faculty of Pharmacy and Food Sciences, Institute of Nutrition and Food Safety (INSA-UB), University of Barcelona, 08028 Barcelona, Spain; naye.yerena@gmail.com (A.L.-Y.); avallverdu@ub.edu (A.V.-Q.); lamuela@ub.edu (R.M.L.-R.)
2 CIBER Physiopathology of Obesity and Nutrition (CIBEROBN), Institute of Health Carlos III, 28029 Madrid, Spain
3 Scientific and Technological Center of University of Barcelona (CCiTUB), 08028 Barcelona, Spain; ojauregui@ccit.ub.edu
4 Biopharmaceutics and Pharmacokinetics Unit, Department of Pharmacy and Pharmaceutical Technology and Physical Chemistry, Institute of Nanoscience and Nanotechnology (IN2UB), Faculty of Pharmacy and Food Sciences, University of Barcelona, 08028 Barcelona, Spain; xgarciasala@ub.edu
5 Pharmaceutical Nanotechnology Group I+D+I Associated Unit to CSIC, University of Barcelona, 08028 Barcelona, Spain
* Correspondence: eescribano@ub.edu; Fax: +34-9340-35937

Abstract: Claims for the potential health benefits of oleocanthal (OLC), a dietary phenolic compound found in olive oil, are based mainly on in vitro studies. Little is known about the tissue availability of OLC, which is rapidly metabolized after ingestion. In this study, the distribution of OLC and its metabolites in rat plasma and tissues (stomach, intestine, liver, kidney, spleen, lungs, heart, brain, thyroid and skin) at 1, 2 and 4.5 h after the acute intake of a refined olive oil containing 0.3 mg/mL of OLC was examined by LC-ESI-LTQ-Orbitrap-MS. OLC was only detected in the stomach and intestine samples. Moreover, at 2 and 4.5 h, the concentration in the stomach decreased by 36% and 74%, respectively, and in the intestine by 16% and 33%, respectively. Ten OLC metabolites arising from phase I and phase II reactions were identified. The metabolites were widely distributed in rat tissues, and the most important metabolizing organs were the small intestine and liver. The two main circulating metabolites were the conjugates OLC + OH + CH_3 and OLC + H_2O + glucuronic acid, which may significantly contribute to the beneficial health effects associated with the regular consumption of extra virgin olive oil. However, more studies are necessary to determine the concentrations and molecular structures of OLC metabolites in human plasma and tissues when consumed with the presence of other phenolic compunds present in EVOO.

Keywords: extra virgin olive oil; polyphenols; metabolism; bioaccumulation; LC-ESI-LTQ-Orbitrap

Citation: López-Yerena, A.; Vallverdú-Queralt, A.; Jáuregui, O.; Garcia-Sala, X.; Lamuela-Raventós, R.M.; Escribano-Ferrer, E. Tissue Distribution of Oleocanthal and Its Metabolites after Oral Ingestion in Rats. *Antioxidants* **2021**, *10*, 688. https://doi.org/10.3390/antiox10050688

Academic Editors: Joanna Oracz and Dorota Żyżelewicz

Received: 8 April 2021
Accepted: 25 April 2021
Published: 27 April 2021

1. Introduction

According to the World Health Organization (WHO), the main causes of death worldwide in 2016 were ischemic heart disease, stroke, chronic obstructive pulmonary disease, lower respiratory infections, Alzheimer's disease and other dementias and diabetes mellitus [1]. In 2018, the Mediterranean diet, a model of eating based on the traditional foods and drinks of the countries surrounding the Mediterranean Sea [2], was recommended by the WHO for its numerous health benefits, including effectiveness in reducing non-communicable diseases [3]. The main source of fat in the Mediterranean diet is extra virgin olive oil (EVOO), whose minority compounds include phenolic substances such as phenolic acids, phenolic alcohols, flavonoids, secoiridoids and lignans [4,5]. Among the secoiridoids, which contain elenolic acid or its derivatives in their molecular structures [6], oleocanthal (OLC) has proven biological activity, including antioxidant and antimicrobial

properties [7,8], anti-inflammatory effects (more potent than ibuprofen) [9], anticancer properties (melanoma, breast, liver and colon cancer and leukemia) [10–12] and neuroprotective effects [13,14].

Recognized by the human body as xenobiotics, phenolic compounds have a relatively low bioavailability compared with micro and macronutrients [15]. Bioavailability depends on multiple factors, including gastrointestinal digestion, absorption and metabolism, as well as tissue distribution [16], which plays a fundamental role in the pharmacokinetic behavior of drugs and other xenobiotics and conditions the pharmacological and toxicological responses of the organism [17]. Studies in animal models help to determine the tissue distribution and accumulation of compounds and their metabolites and identify potential sites of action [18]. To date, the extensive research on the bioavailability of phenolic compounds from EVOO has focused mainly on absorption or metabolism in humans [19–24] and rats [25–28]. Regarding OLC, a low intestinal absorption (16%) and intestinal metabolism in vivo, indicating limited systemic exposure, has been described by only one study [29], whereas none of the investigations aiming to understand the bioavailability of EVOO phenolic compounds have explored OLC tissue distribution. Recently, the OLC reactivity with amino acids with high preference to glycine was also reported [30].

It should also be noted that most of the in vitro studies on the health benefits of OLC do not take into account the matrix, the biological concentrations usually achieved when following a Mediterranean diet, metabolic transformations or the contemporary presence of more than one metabolite [31]. The current work is therefore an attempt to improve our understanding of the health effects of OLC through a tissue distribution study in rats after the oral administration of OLC-enriched refined olive oil (ROO). The distribution of OLC metabolites in multiple tissues and at different times post-administration was also evaluated.

2. Materials and Methods

2.1. Reagents and Materials

OLC (purity > 90) was purchased from PhytoLab GmbH (Vestenbergsgreuth, Germany), and its purity was verified by ^{1}H NMR, as in a previous study [32]. The reagents of methanol, acetonitrile (ACN) and formic acid were purchased from Sigma-Aldrich. Ultrapure water was obtained using a Milli-Q purification system (Millipore, Bedford, MA, USA).

2.2. Animals and Diets

The studies were conducted following a protocol approved by the Animal Experimentation Ethics Committee of the University of Barcelona, Spain (trial no. CEEA 124/16) and Generalitat de Catalunya (no. 6435). Male Sprague Dawley rats (body weight 249 ± 8 g) were purchased from Envigo RMS Spain S.L. (Sant Feliu de Codines, Barcelona, Spain). The animals were acclimatized in animal housing in an air-conditioned room at 22 ± 2 °C under a 12 h/12 h cycle of light and darkness and given free access to a commercial diet (Teklad 2014, Envigo RMS Spain S.L.) and water for at least 10 days before the study. The rats were fasted for over 12 h before the experiments but were allowed free access to water.

2.3. Tissue Distribution Experiments

Before the distribution experiment, the ROO (vehicle) was analyzed by LC-ESI-LTQ-Orbitrap-MS to make sure it was free of phenolic compounds. The liquid–liquid extraction of phenolic compounds of ROO was performed following the previously described procedures [33]. The chromatographic and mass spectrometer conditions were the same as those used for the identification of metabolites (Section 2.3). After verifying that the ROO was free of phenols, OLC was added to obtain a final concentration of 0.3 mg/mL. The OLC concentration was chosen while taking into account both the OLC concentration in commercial EVOO (~300 mg/kg) and the daily ingestion of EVOO recommended by the

European Food Safety Authority of at least 5 mg of hydroxytyrosol and its derivatives per 20 g of olive oil [34].

The rats were divided into four groups—a control group (no administration) and three dosed groups—to study the distribution of OLC at three different time points: 1, 2 and 4.5 h post-administration. On treatment day, the rats received the ROO containing OLC by oral gavage (2.5 mL/300 g body weight). The volume for gavage administration was established following a good practice guide for substance administration [35] and was lower than the maximum volume of lipid vehicles per kg of rat body weight that prevented elevated plasma corticosterone levels [36].

The rats were anesthetized with isoflurane (IsoFloR, Veterinaria Esteve, Barcelona, Spain) and euthanized by exsanguination via cardiac puncture at 1, 2 or 4.5 h after ROO ingestion. The control group was maintained under fasting conditions without olive oil ingestion and then similarly euthanized. The blood was collected in EDTA tubes, and plasma samples were obtained by centrifugation (3000× *g* for 10 min at 4 °C) and stored at −80 °C until analysis. Different tissues and organs (heart, liver, spleen, lungs, kidney, brain, thyroid, stomach, small intestine and skin) were removed from the rats and placed in pre-weighed tubes. The small intestine samples consisted of a pool of duodenum, jejunum and ileum segments, but the main region used was the jejunum. The procedure was to locate the plica duodenocolica [37] and, from there up to about 5 cm of the intestine before reaching the cecum, to remove it from the animal. The collected tissues were washed with physiological serum at 37 °C and placed between absorbent paper to remove the rest of the serum. In the case of the intestine, the luminal contents were first removed by applying pressure with the index finger and thumb, and then the lumen was washed by perfusing with the physiological serum at 37 °C. It was then placed between absorbent paper to remove the remains of the washings. In order to avoid compound oxidation, the collected tissues were kept on ice at all times. Finally, the samples were weighed and stored at −80 °C until analysis. For each group, four animals were used.

2.4. Liquid–Liquid Extraction for Bioanalysis

The tissues were homogenized with a small tissue disruptor (T 10 basic ULTRA-TURRAX®, IKA laboratory technology, Staufen Germany) in a 1:1 ratio (*w*/*v*) with water:ACN (1:1 (*v*/*v*) with 0.1% ascorbic acid). The samples were sonicated for 5 min in an ice bath and shaken for 1 min (Vortex-Genie 2). Each homogenate was centrifuged for 10 min (11,000× *g* at 4 °C). A volume of 100 µL of the upper layer was blended with cold ACN containing 2% formic acid in a 1:3 ratio (*v*/*v*) in order to precipitate the proteins [38]. The samples were homogenized for 1 min and kept at −20 °C for 20 min before centrifugation (11,000× *g* at 4 °C for 10 min). Finally, 100 µL of supernatant was transferred to vials for analysis. Three replicates were evaluated for each sample.

The plasma samples were thawed and centrifuged (11,000× *g* at 4 °C at 10 min). Plasma (100 µL) was mixed with cold ACN containing 2% formic acid in a ratio of 1:5 (*v*/*v*) to precipitate proteins, homogenized for 1 min and kept at −20 °C for 20 min. The samples were then centrifuged (11,000× *g* at 4 °C for 10 min), and finally, 100 µL of each organic phase was transferred to vials for analysis. Three replicates were evaluated for each sample.

2.5. LC-ESI-LTQ-Orbitrap-MS Equipment and Conditions

The LC system consisted of an Accela chromatograph (Thermo Scientific, Hemel Hempstead, UK) with a quaternary pump, a photodiode array detector (PDA) and a thermostated autosampler. The separations were carried out on an Acquity™ UPLC® BEH C_{18} pre-column (2.1 × 5 mm, i.d., 1.7 µm particle size) and an Acquity™ UPLC® BEH C_{18} column (2.1 × 100 mm, i.d., 1.7 µm particle size) (Waters Corporation®, Ireland). The mobile phases consisted of H_2O (A) and methanol (B), both with 0.05% of formic acid. The elution was performed by means of an increasing linear gradient (*v*/*v*) of B (t (min), %B), as follows: (0, 0); (2, 0); (6, 53.6); (8, 100); (9, 100); (9.1, 0); and (11, 0). The injection volume was 5 µL, the flow rate was set to 0.6 mL/min, and the column temperature was 50 °C.

An LTQ Orbitrap Velos mass spectrometer (Thermo Scientific, Hemel Hempstead, UK) equipped with an ESI source in negative mode was used to obtain high-resolution mass spectra for the identification of OLC and its derivatives. The operation parameters were the following: source voltage = 4 kV and capillary temperature = 275 °C (FT automatic gain control (AGC) target 5·105 for MS mode and 5·104 for MSn mode). The sheath gas, auxiliary gas and sweep gas were set at 20, 10 and 2 arbitrary units, respectively. All samples were analyzed in Fourier transform mass spectrometry (FTMS) mode at a resolving power of 30,000 at 600 m/z, and data-dependent MS/MS events were acquired at a resolving power of 15.000 at 600 m/z. The most intense ions detected during FTMS-MS triggered data-dependent scanning. Ions that were not intense enough for a data-dependent scan were analyzed in MSn mode with the same orbitrap resolution (15,000 at 600 m/z). Precursors were fragmented by collision-induced C-trap dissociation with normalized collision energy (35 V) and an activation time of 10 ms. The mass range in FTMS mode was from 100 to 600 m/z. The system was controlled by XCalibur software v2.0.7 (ThermoFisher Scientific).

The OLC calibration curves were prepared in each isolated tissue matrix (heart, liver, spleen, lung, kidney, brain, thyroid, stomach, small intestine and skin) and in plasma (0.1–3 μg/mL). The concentrations of OLC metabolites were calculated using the peak area of the standard OLC and expressed as OLC equivalents. All calibration curves presented R2 > 0.98.

The elemental composition of each metabolite was selected according to the accurate masses and the isotopic pattern (through the Formula Finder feature in XCalibur software v2.0.7 and searched for in the Dictionary of Natural Products (Chapman & Hall/CRC) and the MOTO database (http://appliedbioinformatics.wur.nl/moto, accessed on 23 April 2021). MSn measurements were performed to obtain information on the fragment ions generated in the linear ion trap within the same analysis. Finally, metabolites were confirmed by comparing MS/MS spectra, with fragments reported in the literature as the main tool for the putative identification of OLC [20,24,29].

2.6. Statistical Analysis

Data are presented as the mean and standard deviation (SD). Statistical analysis was performed using SAS (version 9.4). The assumption of normalization was checked with standardized bias and standardized kurtosis. Statistical differences in the concentration of metabolites and OLC at different post-administration times (1, 2 and 4.5 h) for each compound and tissue were evaluated using one-way ANOVA, followed by the LSD post hoc test. Differences were considered significant at $p < 0.05$.

3. Results and Discussion

OLC and its metabolites were not detected in the plasma and tissues of the control group. In the groups receiving ROO, OLC was only detected in the stomach and small intestine samples, with the maximum concentration (C_{max}) being at 1 h of consumption ($p < 0.05$) (Figure 1). In the stomach samples, the concentration decreased by 36% and 74% at 2 h and 4.5 h, respectively, which could be due to gastric emptying and the fact that OLC decomposition increases with gastric residence time, although in the fasted (pH 1.5) and fed (pH 2–3) conditions and normal physiological time frames (up to 4 h), some would remain intact and enter the small intestine unhydrolyzed [39]. The concentration of the OLC that reached the intestine decreased by 16% and 33% at 2 h and 4.5 h post-ingestion, respectively (Figure 1), which can be attributed mainly to the intestinal metabolism and less to intestinal absorption [29].

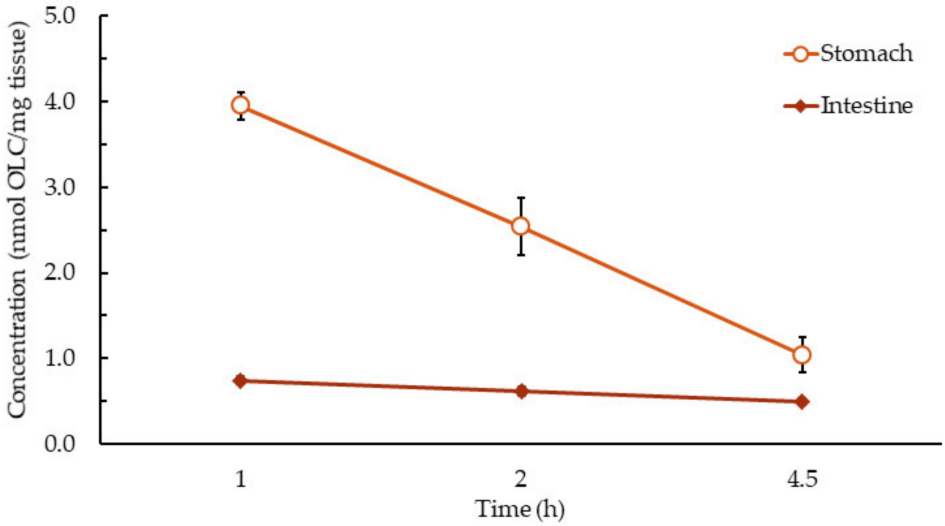

Figure 1. OLC concentrations in the small intestine and stomach (nmol/g tissue), calculated as nmol OLC equivalents. Results are expressed as the mean ± standard deviation.

3.1. Metabolite Identification

Ten metabolites arising from phase I and phase II reactions were identified in the rat plasma and tissues. Accurate and comprehensive identification by LC-ESI-LTQ-Orbitrap-MS showed that the OLC metabolites were widely distributed in different tissues. The corresponding molecular formulas, MS/MS fragments, mass measurement errors and retention times are shown in the Supporting Information (S1). In addition, an example of a chromatogram for each metabolite and the parent compound is shown in Figure S1.

3.1.1. Phase I Metabolism

The first step in the digestion of dietary lipids in the stomach involves their dispersal into finely divided emulsion particles, generating a lipid–water interface [40]. Previous studies have demonstrated that phenolic compounds are transferred to the aqueous or oily phase according to their polarity [41]. In the case of OLC, its amphiphilic characteristics result in a partition between the oily and aqueous phase, tending toward a higher concentration in the latter (68.7%) due to its polar functional groups [42]. At the same time, OLC can be partially modified in the acidic environment of the stomach, where OLC was hydrolyzed into tyrosol (TY) and only detected in the stomach and intestinal samples, with the highest concentrations observed at 1 h of intragastric administration (Figure 2A). Reports on secoiridoid hydrolysis in the literature are contradictory. Thus, whereas in vitro and in vivo studies described secoiridoid compounds undergoing a rapid hydrolysis under gastric conditions, leading to an increase in hydroxytyrosol and TY concentrations [24,41], an in vitro digestion study observed good OLC stability in the gastric phase [42]. According to our results, the hydrolysis of OLC can occur due to either acidic conditions or the presence of nonlipolytic carboxylic ester hydrolases, which hydrolyze carboxylic esters cleaved into an acid and an alcohol [43]. In our study, the observation of TY in samples of the stomach and intestine but not the other organs can be attributed to its metabolization by enzymes of the gastrointestinal mucosal epithelium before entering the systemic circulation. However, TY metabolites were not detected, possibly because they were at a very low concentration.

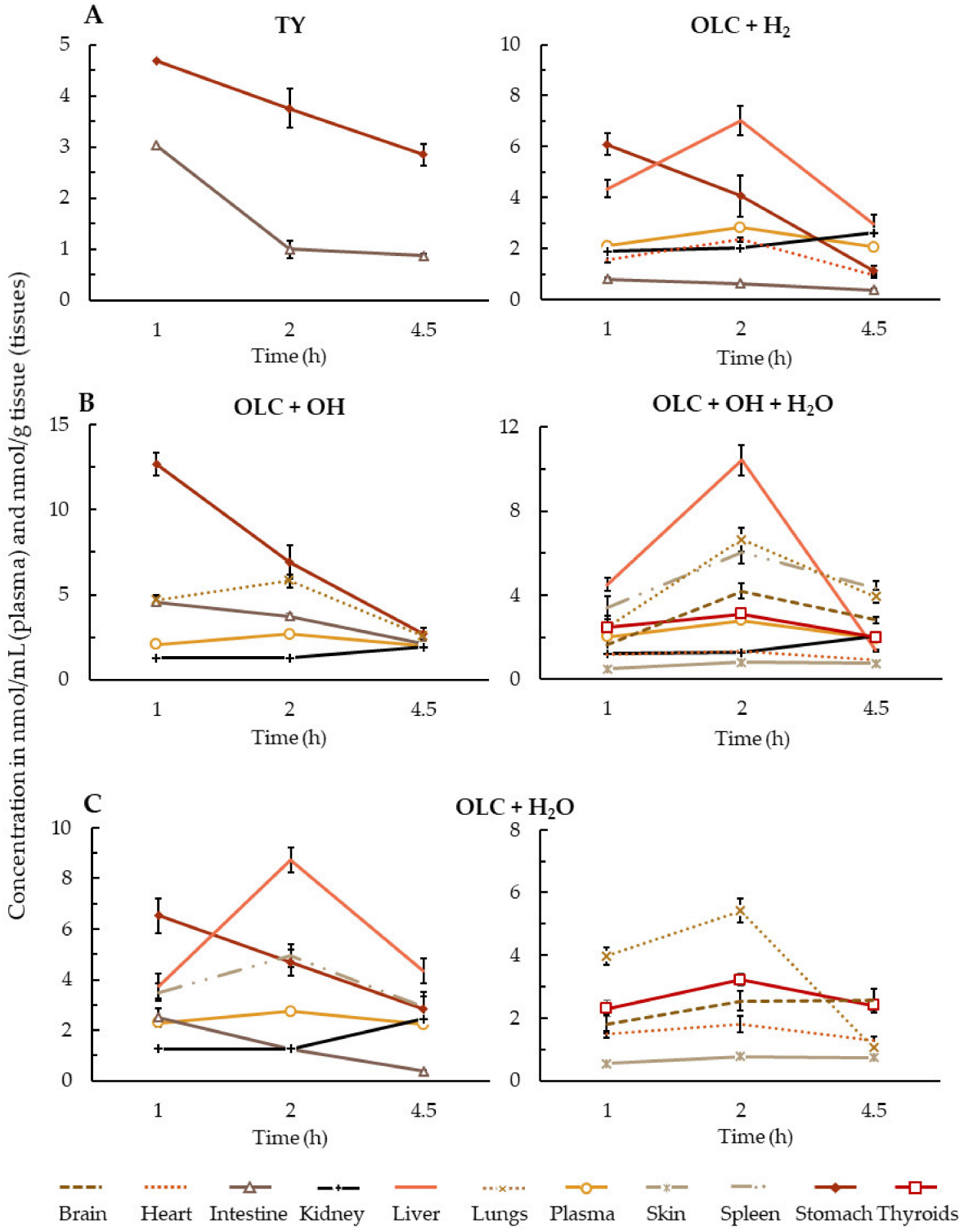

Figure 2. Phase I metabolites of OLC in plasma (nmol/mL) and tissues (nmol/g tissue), calculated as nmol OLC equivalents. (**A**): TY and OLC + H_2 metabolites; (**B**): OLC + OH and OLC + OH + H_2O metabolites; (**C**): OLC + H_2O metabolite. Results are expressed as the mean ± standard deviation.

Non-hydrolyzed OLC in the acidic conditions of the stomach can undergo different phase I biotransformations. The metabolite OLC + H_2 was identified in the plasma, stomach, intestine, liver, kidney and heart samples (Figure 2A), with a C_{max} (the highest concentration observed among the three evaluation sample times) in the plasma, liver and

heart at 2 h of ROO intake ($p < 0.05$), in the stomach and small intestine at 1 h and in the kidney at 4.5 h. In another study, small traces of OLC + H_2 were detected in human urine at 2 h after a high intake of olive oil [20]. Recently, the same metabolite was identified in the plasma and lumen samples in an intestinal perfusion study in rats [29], whereas it was not found in a screening of secoiridoid metabolites in humans after an acute intake of EVOO [24]. Recently, it was suggested that the reduction OLC is catalyzed by NADPH-dependent aldo-keto reductases (AKR) located in the small intestine epithelium, and it can occur because OLC contains an open dialdehydic form of the attached elenolic acid molecule [29].

A hydroxylated metabolite, OLC + OH, was found in the plasma, stomach, intestine, kidney and lungs (Figure 2B). The C_{max} in the stomach and small intestine samples was at 1 h, at 2 h in the plasma and at 4.5 h in the lungs and in the kidney ($p < 0.05$). Only one previous study [29] has identified this metabolite in rat plasma and lumen samples, while in another it was reported in human urine, although there were doubts about whether it was in fact a hydroxytyrosol derivative such as oleacein [20]. In our study, OLC + OH was not detected in the main metabolizing organ, the liver, where it would have rapidly undergone other metabolic reactions, such as the addition of another OH group, methylation or glucuronidation. Its presence in the plasma, lungs and the brain could be due to enzymatic deconjugation, which occurs with glucuronidated metabolites of quercetin [44] or hydroxytyrosol [45].

The only metabolite present in all the samples was the hydrated form of OLC (Figure 2C). The C_{max} in the stomach and small intestine was at 1 h, in the kidney at 4.5 h ($p < 0.05$), in the brain and skin at 2 h and 4.5 h (the differences were insignificant) and in the plasma and the rest of the tissues at 2 h post-ingestion. Other studies have reported this metabolite in plasma [24,29].

A new OLC metabolite, OLC + OH + H_2O, which was not previously reported in either human or animal experiments [20,23–25,29], was identified in all tissues except the stomach and small intestine (Figure 2B). The C_{max} in most of the samples was at 2 h post-consumption of ROO, at 4.5 h in the kidney and at both 2 h and 4.5 h in the skin. This metabolite could be formed from the hydroxylated and hydrated metabolites identified in the stomach and small intestine following further metabolic reactions in the liver (+ OH or + H_2O). In our study, the presence of OLC + OH + H_2O could be attributed to the hepatic expression of CYP enzymes responsible for the majority of phase I-dependent drug metabolism and for the metabolism of a huge variety of dietary constituents and endogenous chemicals [46].

In the stomach, small intestine and liver [47,48], CYP functions act as a barrier against drugs and chemical compounds, catalyzing and introducing an oxygen atom into substrate molecules, which often results in dealkylated and hydroxylated metabolites [48].

3.1.2. Phase II Metabolism

OLC that escapes first-pass metabolism and the phase I metabolites can undergo other biotransformations. Our results suggest that the hydroxylated (OLC + OH) and hydrated (OLC + H_2O) forms of OLC were subject to the addition of a methyl group (OLC + OH + CH_3 and OLC + H_2O + CH_3). Catechol-O-methyltransferases (COMT) are conjugating enzymes that catalyze the transfer of a methyl group from *S*-adenosyl-L-methionine to phenolic compounds with an O-diphenolic moiety. This reaction usually takes place at the 3´position of the compound, although a minor proportion of 4´-O-methylated product is also possible [49]. OLC + OH + CH_3 was the only conjugated metabolite detected in all analyzed tissues (Figure 3A). The COMT enzymes are most active in the liver and kidneys but are also active in the pylorus of the stomach and in the small intestine, especially the duodenum and ileum [50], a behavior that would explain the presence of this conjugated metabolite in our samples. In contrast, OLC + H_2O + CH_3 was found in almost all samples, except in the stomach and intestine, probably due to the high activity of COMT enzymes in the liver. The C_{max} of both conjugated OLC derivatives (OLC + OH + CH_3 and OLC +

$H_2O + CH_3$) in the plasma and most of the tissues (liver, spleen, hearts, lungs and thyroids) were reached at 2 h after ROO ingestion ($p < 0.05$) and at 4.5 h in the kidney ($p < 0.05$). In the skin, the C_{max} was reached at 2 h and with a similar concentration at 4.5 h ($p > 0.05$). The only previous study to determine the intestinal metabolic profile of OLC did not detect either of these metabolites [29], whereas other in vivo studies observed the same trend found here [20,23–25].

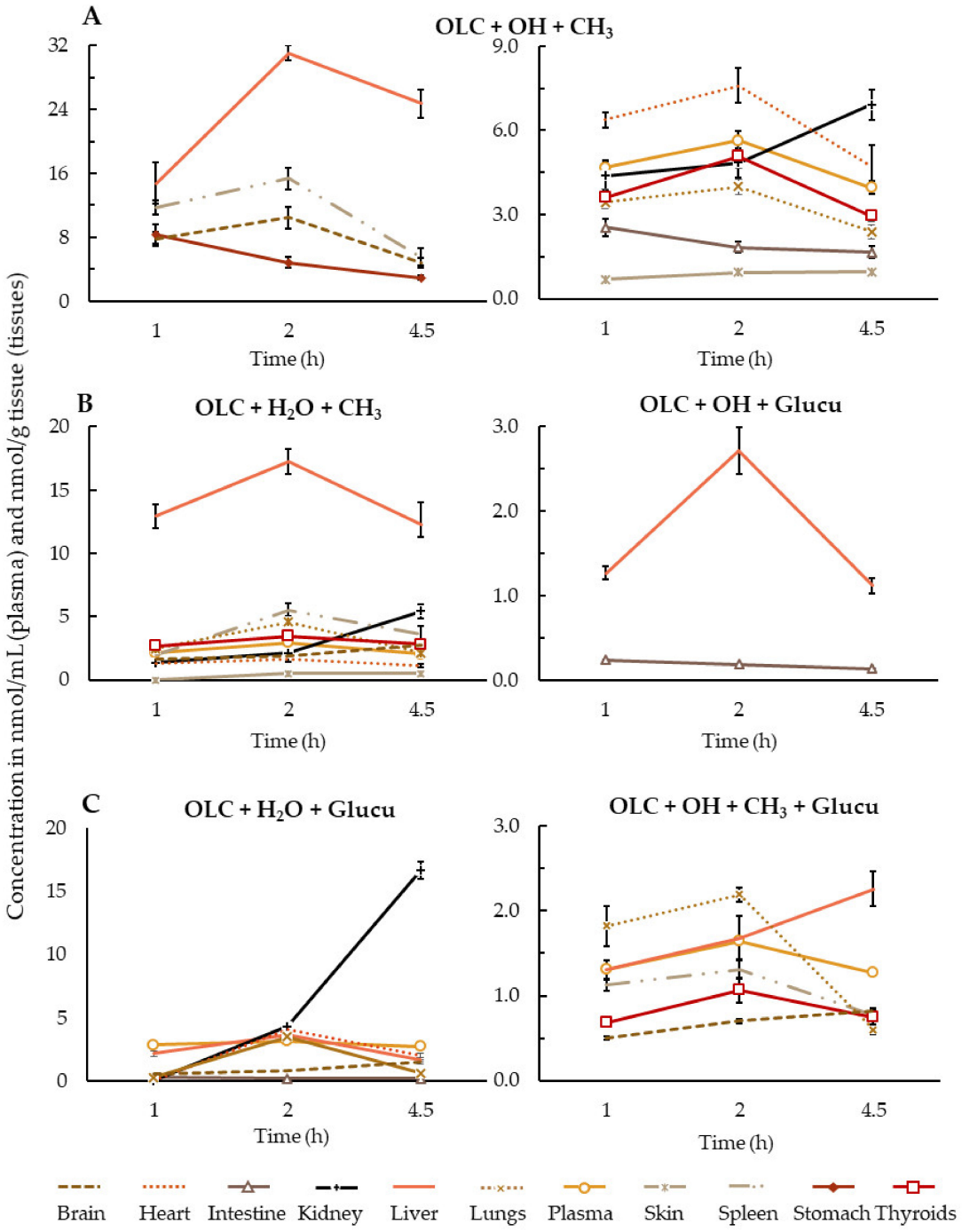

Figure 3. Phase II metabolites in plasma (nmol/mL) and tissues (nmol/g tissue), calculated as nmol OLC equivalents. (**A**): OLC + OH + CH_3 metabolite; (**B**): OLC + H_2O + CH_3 and OLC + OH + glucuronidation metabolites; (**C**): OLC + H_2O + glucuronidation and OLC + OH + CH_3 + glucuronidation metabolites. Results are expressed as the mean ± standard deviation.

A frequent phase II reaction is catalyzed by uridine-disphosphate glucuronosyl transferase (UGT), an enzyme located in the endoplasmic reticulum that mediates the transfer of glucuronic acid from uridine diphosphate to lipophilic compounds [51]. It is known that UGT interacts with structures that have one glucuronidation site and two hydrophobic sites separated by 3 or 6.2 Å of aliphatic hydroxyls, carboxylic acid and amines [52,53]. Although the liver is the main site of glucuronidation [54], there is clear evidence for the expression of UGT in the stomach [54], and UGT1A8 and UGT1A10 are exclusively expressed in the small intestine [53]. Figure 3 also shows the metabolites containing a glucuronic acid. OLC + OH + glucu was only detected in the small intestine, where UGT enzymes are expressed, and the liver (Figure 3B). The C_{max} in the small intestine was at 1 h after ROO intake, and in the liver, it was at 2 h ($p < 0.05$). In contrast, OLC + H_2O + glucu was more widespread (Figure 3C), with a C_{max} in the small intestine at 1 h of ROO intake, at 2 h in the plasma, liver, heart and lungs and at 4.5 h in the kidney and brain ($p < 0.05$). OLC + H_2O + CH_3 or OLC + H_2O + glucu underwent further metabolization, resulting in OLC + OH + CH_3 + glucu, which was found in the plasma, liver, spleen, lungs, thyroid and brain (Figure 3C). The three phase II metabolites detected in our samples had not been previously identified in rat tissues [25] or human urine [20,22,24] or plasma [23]. In a recent study on OLC absorption, only the OLC + H_2O + glucu metabolite was identified in plasma [29]. Nevertheless, the glucuronidation of OLC, which was not observed here, had been detected in human urine after the intake of EVOO [20,24].

3.2. Brief Summary of OLC Metabolite Distribution by Tissue

Our results show that the OLC metabolites were widely distributed in all the tested tissues, even in the brain and skin (Figures 2 and 3). The liver, small intestine and plasma were the biological samples with the greatest variety of metabolites.

In the stomach samples, in addition to OLC, four metabolites from the phase I reactions and one from the phase II reactions were detected (Figures 2 and 3). The presence of a TY metabolite in the stomach indicates that OLC underwent a rapid hydrolysis under gastric conditions. The C_{max} of all the metabolites was observed at 1 h of ROO intake.

Besides OLC, a wide range of its metabolites was found in the small intestine, where concentrations were lower than in the stomach. It is well known that the small intestine is the main site where xenobiotic absorption occurs [55,56], and the intestinal epithelial membrane is the principle physiological barrier that chemicals must cross to enter the bloodstream [57]. Phenolic compounds can be metabolized in the small intestine by numerous pathways involving both phase I and phase II reactions. Accordingly, four phase I and three phase II derivatives were identified (Figures 2 and 3). For all the metabolites, the C_{max} was observed at 1 h of ROO intake. These results confirm that OLC is subjected to a high intestinal metabolism, as previously reported [29].

According to the results obtained, the liver (in addition to the small intestine) represents the main metabolizing organ for OLC. For most of the metabolites detected in the liver, the C_{max} was at 2 h. Up to five phase II metabolites were found at high concentrations, in accordance with the functionality of this organ in xenobiotic and phenolic compound metabolism. The results are consistent with those obtained in a tissue distribution study in rats after olive cake ingestion, in which the highest number and concentration of metabolites were detected in the liver [25].

OLC was not found in the plasma, which could be explained by its relatively low absorption (16%) and high intestinal metabolism [29]. In the latter study, OLC was detected in mesenteric blood plasma, but the compound was administered directly to the small intestine, thus avoiding passing through the stomach and the liver, where OLC hydrolysis and metabolism can potentially take place, respectively. Although OLC was not detected in the plasma, four phase I and four phase II metabolites were identified in the plasma with a C_{max} at 2 h. This study demonstrates for the first time that OLC + OH + CH_3 is the main circulating OLC metabolite in rats after OLC consumption, followed by OLC + H_2O + glucu. The systemic exposure of these metabolites can reflect tissue exposure [58]. It is worth

noting that most in vitro and in vivo studies or clinical trials determining the effects of OLC have focused on the control and progression of different types of cancer, cardiovascular diseases, neurodegeneration, anti-aging processes and immunoinflammatory diseases, but the biological concentrations of OLC [6,59] and its major circulating metabolites were not considered.

The potential protective effect of OLC againt Alzheimer's disease has been investigated in both in vitro and in vivo studies [13,14,60]. However, for the first time, it was demonstrated that only the metabolites (Figures 2 and 3) were able to cross the blood–brain barrier in rats—at the dose of OLC administered—and undergo brain uptake. The results showed brain accumulation of the OLC + OH + CH_3 metabolite, suggesting that this metabolite could be able to exert beneficial effects, specifically neuroprotective activity, by the reduction of the oxidative stress at the neuronal level. However, in the last decade, several studies have been focused on the evaluation of the potential health benefits of OLC, and the data available about the biological relevance of its metabolites are still limited. Futures studies about the effective brain accumulation of the main biological OLC metabolites are needed to determine their potential to protect neuronal cells.

Based on the number and high concentration of OLC metabolites detected in the lungs, this organ is an important site of extrahepatic OLC metabolism. It is well known that the lungs contain drug-metabolizing enzymes, with low levels of monooxidases, transferases and esterases found in the endothelial cells, which may contribute to the elimination of drugs and xenobiotics [60,61]. A wide range of OLC derivatives (six) were also found in the heart, more than in the spleen and thyroids (5). In all these samples, OLC + OH + CH_3 was the main metabolite detected. Various drug-metabolizing enzymes are also expressed by macrophages and lymphocytes present in the white pulp region of the spleen, explaining the presence of metabolites in this tissue. More information about the metabolite functionality in the spleen is required [25], although a role of the spleen in lipid metabolism has been reported [62].

The wide range of metabolites detected in the kidney indicates that renal excretion is a major pathway of elimination for OLC metabolites in rats. In addition, accumulating evidence indicates that specific CYP, UGT and possibly other drug-metabolizing enzymes contribute to renal drug and chemical metabolic clearance, thereby modulating intrarenal exposure to these compounds, as well as regulating the activity of physiological mediators [63].

Even though the skin was the tissue where the fewest metabolites arrived, this study also contributes to providing a new perspective for understanding how the mechanism through EVOO phenolic compounds acts in the body.

The findings found in this study suppose a breakthrough in the research to understand the positive correlation of olive oil phenolic compound consumption and the prevention and improvement of some diseases. Nevertheless, further experiments are required to investigate the effect of the main circulating metabolites on the functions of the target tissues, such as those in the brain, heart, skin and spleen.

4. Conclusions and Remarks

There is still a lack of information on the distribution and accumulation of olive oil phenolic compounds in the body. In this study, the distribution and accumulation of OLC metabolites in rat tissues was studied for the first time. The results demonstrate that under gastric conditions, OLC was hydrolyzed to TY, whereas the non-hydrolyzed OLC underwent different phase I biotransformations in the stomach and small intestine. Once absorbed, the phase I metabolites were widely distributed throughout the organism or underwent further metabolic reactions. Although OLC was not detected in the tissues, its metabolites were found in the lungs, heart, brain, thyroids, spleen and skin in sufficient concentrations to exert beneficial effects. The main circulating metabolites arising from phase II reactions were OLC + OH + CH_3 and OLC + H_2O + glucu, suggesting that these metabolites are likely to significantly contribute to the beneficial health effects associated

with the regular consumption of olive products. However, more studies are necessary to determine the concentrations and composition of OLC metabolites in human plasma and tissues, as well as pharmacodynamic studies that relate concentrations vs. effects.

Supplementary Materials: The following are available online at https://www.mdpi.com/article/10.3390/antiox10050688/s1, Table S1. Identification of OLC and its metabolites in plasma and tissues through LTQ-Orbitrap-MS. Figure S1. Extracted ion chromatograms of the OLC and its identified metabolites in different tissues.

Author Contributions: Conceptualization, A.L.-Y., E.E.-F. and R.M.L.-R.; methodology, A.L.-Y., E.E.-F., O.J. and A.V.-Q.; software, A.L.-Y., E.E.-F. and A.V.-Q.; validation, A.L.-Y., E.E.-F. and R.M.L.-R.; formal analysis, A.L.-Y. and E.E.-F.; investigation, A.L.-Y. and E.E.-F.; resources, R.M.L.-R.; data curation, A.L.-Y., E.E.-F., O.J. and A.V.-Q.; writing—original draft preparation, A.L.-Y. and E.E.-F.; writing—review and editing, A.L.-Y., X.G.-S. and E.E.-F.; visualization, A.L.-Y., X.G.-S. and E.E.-F.; supervision, E.E.-F. and R.M.L.-R.; project administration, E.E.-F. and R.M.L.-R. All authors have read and agreed to the published version of the manuscript.

Funding: This research was funded by CICYT [AGL2016-75329-R], CIBEROBN from the Instituto de Salud Carlos III, ISCIII from the Ministerio de Ciencia, Innovación y Universidades, (AEI/FEDER, UE) and Generalitat de Catalunya (GC) [2017SGR 196]. A.L.-Y. wishes to thank the Consejo Nacional de Ciencia y Tecnología (CONACYT) of Mexico for the doctoral scholarship. A.V.-Q. thanks the Ministry of Science Innovation and Universities for the Ramon y Cajal contract (RYC-2016-19355).

Institutional Review Board Statement: The studies were conducted following a protocol approved by the Animal Experimentation Ethics Committee of the University of Barcelona, Spain (trial no. CEEA 124/16) and Generalitat de Catalunya (no. 6435).

Informed Consent Statement: Not applicable.

Data Availability Statement: Data is contained within the article or supplementary material. The data presented in this study are available in Figures 1–3.

Acknowledgments: The authors wish to thank the CCiT-UB for the mass spectrometry equipment.

Conflicts of Interest: R.M.L.-R. reports receiving lecture fees from Cerveceros de España and receiving lecture fees and travel support from Adventia. The other authors declare no conflict of interest. The funders had no role in the design of the study; in the collection, analyses, or interpretation of data; in the writing of the manuscript, or in the decision to publish the results.

References

1. World Health Organisation. The Top 10 Causes of Death. Available online: https://www.who.int/en/news-room/fact-sheets/detail/the-top-10-causes-of-death (accessed on 9 December 2020).
2. Dinu, M.; Pagliai, G.; Casini, A.; Sofi, F. Mediterranean Diet and Multiple Health Outcomes: An Umbrella Review of Meta-Analyses of Observational Studies and Randomised Trials. *European J. Clin. Nutr.* **2018**, *72*, 30–43. [CrossRef]
3. Renzella, J.; Townsend, N.; Jewell, J.; Breda, J.; Roberts, N.; Rayner, M.; Wickramasinghe, K. What National and Subnational Interventions and Policies Based on Mediterranean and Nordic Diets Are Recommended or Implemented in the WHO European Region, and Is There Evidence of Effectiveness in Reducing Noncommunicable Diseases. World Health Organization, Regional Office for Europe: Geneva, Switzerland, 2018; ISBN 92-890-5301-1.
4. Romani, A.; Ieri, F.; Urciuoli, S.; Noce, A.; Marrone, G.; Nediani, C.; Bernini, R. Health Effects of Phenolic Compounds Found in Extra-Virgin Olive Oil, By-Products, and Leaf of Olea Europaea L. *Nutrients* **2019**, *11*, 1776. [CrossRef] [PubMed]
5. Piroddi, M.; Albini, A.; Fabiani, R.; Giovannelli, L.; Luceri, C.; Natella, F.; Rosignoli, P.; Rossi, T.; Taticchi, A.; Servili, M.; et al. Nutrigenomics of Extra-Virgin Olive Oil: A Review. *BioFactors* **2017**, *43*, 17–41. [CrossRef] [PubMed]
6. Lozano-Castellón, J.; López-Yerena, A.; Rinaldi de Alvarenga, J.F.; Romero del Castillo-Alba, J.; Vallverdú-Queralt, A.; Escribano-Ferrer, E.; Lamuela-Raventós, R.M. Health-Promoting Properties of Oleocanthal and Oleacein: Two Secoiridoids from Extra-Virgin Olive Oil. *Crit. Rev. Food Sci. Nutr.* **2020**, *60*, 2532–2548. [CrossRef]
7. Nikou, T.; Liaki, V.; Stathopoulos, P.; Sklirou, A.D.; Tsakiri, E.N.; Jakschitz, T.; Bonn, G.; Trougakos, I.P.; Halabalaki, M.; Skaltsounis, L.A. Comparison Survey of EVOO Polyphenols and Exploration of Healthy Aging-Promoting Properties of Oleocanthal and Oleacein. *Food Chem. Toxicol.* **2019**, *125*, 403–412. [CrossRef]
8. Cicerale, S.; Lucas, L.J.; Keast, R.S.J. Antimicrobial, Antioxidant and Anti-Inflammatory Phenolic Activities in Extra Virgin Olive Oil. *Curr. Opinion Biotechnol.* **2012**, *23*, 129–135. [CrossRef] [PubMed]
9. Beauchamp, G.K.; Keast, R.S.J.; Morel, D.; Lin, J.; Pika, J.; Han, Q.; Lee, C.-H.; Smith, A.B.; Breslin, P.A.S. Ibuprofen-like Activity in Extra-Virgin Olive Oil. *Nature* **2005**, *437*, 45–46. [CrossRef]

10. LeGendre, O.; Breslin, P.A.S.; Foster, D.A. (-)-Oleocanthal Rapidly and Selectively Induces Cancer Cell Death via Lysosomal Membrane Permeabilization. *Mol. Cell. Oncol.* **2015**, *2*. [CrossRef]
11. Khanfar, M.A.; Bardaweel, S.K.; Akl, M.R.; El Sayed, K.A. Olive Oil-Derived Oleocanthal as Potent Inhibitor of Mammalian Target of Rapamycin: Biological Evaluation and Molecular Modeling Studies. *Phytother. Res.* **2015**, *29*, 1776–1782. [CrossRef]
12. Siddique, A.B.; Ebrahim, H.Y.; Akl, M.R.; Ayoub, N.M.; Goda, A.A.; Mohyeldin, M.M.; Nagumalli, S.K.; Hananeh, W.M.; Liu, Y.Y.; Meyer, S.A.; et al. (−)-Oleocanthal Combined with Lapatinib Treatment Synergized against HER-2 Positive Breast Cancer in Vitro and in Vivo. *Nutrients* **2019**, *11*, 412. [CrossRef]
13. Qosa, H.; Batarseh, Y.S.; Mohyeldin, M.M.; El Sayed, K.A.; Keller, J.N.; Kaddoumi, A. Oleocanthal Enhances Amyloid-β Clearance from the Brains of TgSwDI Mice and in Vitro across a Human Blood-Brain Barrier Model. *ACS Chem. Neurosci.* **2015**, *6*, 1849–1859. [CrossRef]
14. Monti, M.C.; Margarucci, L.; Riccio, R.; Casapullo, A. Modulation of Tau Protein Fibrillization by Oleocanthal. *J. Nat. Prod.* **2012**, *75*, 1584–1588. [CrossRef] [PubMed]
15. Oracz, J.; Nebesny, E.; Zyzelewicz, D.; Budryn, G.; Luzak, B. Bioavailability and Metabolism of Selected Cocoa Bioactive Compounds: A Comprehensive Review. *Crit. Rev. Food Sci. Nutr.* **2019**, 1–39. [CrossRef]
16. Angelino, D.; Cossu, M.; Marti, A.; Zanoletti, M.; Chiavaroli, L.; Brighenti, F.; Del Rio, D.; Martini, D. Bioaccessibility and Bioavailability of Phenolic Compounds in Bread: A Review. *Food Funct.* **2017**, *8*, 2368–2393. [CrossRef] [PubMed]
17. Lanao, J.; Fraile, M. Drug Tissue Distribution: Study Methods and Therapeutic Implications. *Curr. Pharm. Des.* **2005**, *11*, 3829–3845. [CrossRef] [PubMed]
18. Singh, G. Preclinical Drug Development. In *Pharmaceutical Medicine and Translational Clinical Research*; Academic Press: Waltham, MA, USA, 2017; ISBN 9780128021033.
19. de Bock, M.; Thorstensen, E.B.; Derraik, J.G.B.; Henderson, H.V.; Hofman, P.L.; Cutfield, W.S. Human Absorption and Metabolism of Oleuropein and Hydroxytyrosol Ingested as Olive (*Olea Europaea* L.) Leaf Extract. *Mol. Nutr. Food Res.* **2013**, *57*, 2079–2085. [CrossRef] [PubMed]
20. García-Villalba, R.; Carrasco-Pancorbo, A.; Nevedomskaya, E.; Mayboroda, O.A.; Deelder, A.M.; Segura-Carretero, A.; Fernández-Gutiérrez, A. Exploratory Analysis of Human Urine by LC–ESI-TOF MS after High Intake of Olive Oil: Understanding the Metabolism of Polyphenols. *Anal. Bioanal. Chem.* **2010**, *398*, 463–475. [CrossRef] [PubMed]
21. Rubió, L.; Farràs, M.; de La Torre, R.; Macià, A.; Romero, M.-P.; Valls, R.M.; Solà, R.; Farré, M.; Fitó, M.; Motilva, M.-J. Metabolite Profiling of Olive Oil and Thyme Phenols after a Sustained Intake of Two Phenol-Enriched Olive Oils by Humans: Identification of Compliance Markers. *Food Res. Int.* **2014**, *65*, 59–68. [CrossRef]
22. Khymenets, O.; Farré, M.; Pujadas, M.; Ortiz, E.; Joglar, J.; Covas, M.I.; de la Torre, R. Direct Analysis of Glucuronidated Metabolites of Main Olive Oil Phenols in Human Urine after Dietary Consumption of Virgin Olive Oil. *Food Chem.* **2011**, *126*, 306–314. [CrossRef]
23. Suárez, M.; Valls, R.M.; Romero, M.-P.; Macià, A.; Fernández, S.; Giralt, M.; Solà, R.; Motilva, M.-J. Bioavailability of Phenols from a Phenol-Enriched Olive Oil. *Br. J. Nutr.* **2011**, *106*, 1691–1701. [CrossRef]
24. Silva, S.; Garcia-aloy, M.; Figueira, M.E.; Combet, E.; Mullen, W.; Ros, M. High Resolution Mass Spectrometric Analysis of Secoiridoids and Metabolites as Biomarkers of Acute Olive Oil Intake — An Approach to Study Interindividual Variability in Humans. *Mol. Nutr. Food Res.* **2018**, *1700065*. [CrossRef] [PubMed]
25. Serra, A.; Rubió, L.; Borràs, X.; Macià, A.; Romero, M.-P.; Motilva, M.-J. Distribution of Olive Oil Phenolic Compounds in Rat Tissues after Administration of a Phenolic Extract from Olive Cake. *Mol. Nutr. Food Res.* **2012**, *56*, 486–496. [CrossRef]
26. Pinto, J.; Paiva-Martins, F.; Corona, G.; Debnam, E.S.; Jose Oruna-Concha, M.; Vauzour, D.; Gordon, M.H.; Spencer, J.P.E. Absorption and Metabolism of Olive Oil Secoiridoids in the Small Intestine. *Br. J. Nutr.* **2011**, *105*, 1607–1618. [CrossRef]
27. López de las Hazas, M.-C.; Piñol, C.; Macià, A.; Romero, M.-P.; Pedret, A.; Solà, R.; Rubió, L.; Motilva, M.-J. Differential Absorption and Metabolism of Hydroxytyrosol and Its Precursors Oleuropein and Secoiridoids. *J. Funct. Foods* **2016**, *22*, 52–63. [CrossRef]
28. Domínguez-Perles, R.; Auñón, D.; Ferreres, F.; Gil-Izquierdo, A. Gender Differences in Plasma and Urine Metabolites from Sprague–Dawley Rats after Oral Administration of Normal and High Doses of Hydroxytyrosol, Hydroxytyrosol Acetate, and DOPAC. *Eur. J. Nutr.* **2017**, *56*, 215–224. [CrossRef]
29. López-Yerena, A.; Vallverdú-Queralt, A.; Mols, R.; Augustijns, P.; Lamuela-Raventós, R.M.; Escribano-Ferrer, E. Absorption and Intestinal Metabolic Profile of Oleocanthal in Rats. *Pharmaceutics* **2020**, *12*, 134. [CrossRef]
30. Darakjian, L.I.; Rigakou, A.; Brannen, A.; Qusa, M.H.; Tasiakou, N.; Diamantakos, P.; Reed, M.N.; Panizzi, P.; Boersma, M.D.; Melliou, E.; et al. Spontaneous In Vitro and In Vivo Interaction of (−)-Oleocanthal with Glycine in Biological Fluids: Novel Pharmacokinetic Markers. *ACS Pharmacol. Transl. Sci.* **2021**, *4*, 179–192. [CrossRef]
31. Serreli, G.; Deiana, M. In Vivo Formed Metabolites of Polyphenols and Their Biological Efficacy. *Food Funct.* **2019**, *10*, 6999–7021. [CrossRef]
32. López-Yerena, A.; Vallverdú-Queralt, A.; Mols, R.; Augustijns, P.; Lamuela-Raventós, R.M.; Escribano-Ferrer, E. Reply to "Comment on López-Yerena et al. 'Absorption and Intestinal Metabolic Profile of Oleocanthal in Rats' Pharmaceutics 2020, 12, 134.". *Pharmaceutics* **2020**, *12*, 1221. [CrossRef]
33. Lozano-Castellón, J.; López-Yerena, A.; Olmo-Cunillera, A.; Jáuregui, O.; Pérez, M.; Lamuela-Raventós, R.M.; Vallverdú-Queralt, A. Total Analysis of the Major Secoiridoids in Extra Virgin Olive Oil: Validation of an UHPLC-ESI-MS/MS Method. *Antioxidants* **2021**, *10*, 540. [CrossRef]

34. Panel, E.; Nda, A. Scientific Opinion on the Substantiation of Health Claims Related to Polyphenols in Olive and Protection of LDL Particles from Oxidative Damage (ID 1333, 1638, 1639, 1696, 2865), Maintenance of Normal Blood HDL Cholesterol Concentrations (ID 1639), Mainte. *EFSA J.* **2011**, *9*, 1–25. [CrossRef]
35. Diehl, K.-H.; Hull, R.; Morton, D.; Pfister, R.; Rabemampianina, Y.; Smith, D.; Vidal, J.-M.; Vorstenbosch, C.V.D. A Good Practice Guide to the Administration of Substances and Removal of Blood, Including Routes and Volumes. *J. Appl. Toxicol.* **2001**, *21*, 15–23. [CrossRef]
36. Brown, A.P.; Dinger, N.; Levine, B.S. Stress Produced by Gavage Administration in the Rat. *Contemp. Top. Lab. Anim. Sci.* **2000**, *39*, 17–21.
37. Ishida, M.; Sakata, N.; Ise, I.; Ono, T.; Shimura, M.; Ishii, K.; Murakami, M.; Takadate, T.; Aoki, T.; Kudo, K. The Comparative Anatomy of the Folds, Fossae, and Adhesions around the Duodenojejunal Flexure in Mammals. *Folia Morphol.* **2018**, *77*, 286–292. [CrossRef]
38. Polson, C.; Sarkar, P.; Incledon, B.; Raguvaran, V.; Grant, R. Optimization of Protein Precipitation Based upon Effectiveness of Protein Removal and Ionization Effect in Liquid Chromatography–Tandem Mass Spectrometry. *J. Chromatogr. B* **2003**, *785*, 263–275. [CrossRef]
39. Corona, G.; Tzounis, X.; Dessì, M.A.; Deiana, M.; Edward, S.; Visioli, F.; Spencer, J.P.E.; Corona, G.; Tzounis, X.; Dessì, M.A.; et al. The Fate of Olive Oil Polyphenols in the Gastrointestinal Tract: Implications of Gastric and Colonic Microflora-Dependent Biotransformation. *Free Radic. Res.* **2006**, *40*, 647–658. [CrossRef]
40. Singh, H.; Ye, A.; Horne, D. Structuring Food Emulsions in the Gastrointestinal Tract to Modify Lipid Digestion. *Prog. Lipid Res.* **2009**, *48*, 92–100. [CrossRef]
41. Quintero-Flórez, A.; Pereira-Caro, G.; Sánchez-Quezada, C.; Moreno-Rojas, J.M.; Gaforio, J.J.; Jimenez, A.; Beltrán, G. Effect of Olive Cultivar on Bioaccessibility and Antioxidant Activity of Phenolic Fraction of Virgin Olive Oil. *Eur. J. Nutr.* **2017**, 1–22. [CrossRef]
42. Soler, A.; Romero, M.P.; Macià, A.; Saha, S.; Furniss, C.S.M.; Kroon, P.A.; Motilva, M.J. Digestion Stability and Evaluation of the Metabolism and Transport of Olive Oil Phenols in the Human Small-Intestinal Epithelial Caco-2/TC7 Cell Line. *Food Chem.* **2010**, *119*, 703–714. [CrossRef]
43. Yassine Ben, A.; Verger, R.; Abousalham, A. Lipases or Esterases: Does It Really Matter? Toward a New Bio-Physico-Chemical Classification. In *Lipases and Phospholipases*; Humana Press: Totowa, NJ, USA, 2012; pp. 31–51.
44. Menendez, C.; Dueñas, M.; Galindo, P.; González-Manzano, S.; Jimenez, R.; Moreno, L.; Zarzuelo, M.J.; Rodríguez-Gómez, I.; Duarte, J.; Santos-Buelga, C.; et al. Vascular Deconjugation of Quercetin Glucuronide: The Flavonoid Paradox Revealed? *Mol. Nutr. Food Res.* **2011**, *55*, 1780–1790. [CrossRef]
45. Rubió, L.; Serra, A.; Macià, A.; Piñol, C.; Romero, M.-P.; Motilva, M.-J. In Vivo Distribution and Deconjugation of Hydroxytyrosol Phase II Metabolites in Red Blood Cells: A Potential New Target for Hydroxytyrosol. *J. Funct. Foods* **2014**, *10*, 139–143. [CrossRef]
46. Dressman, J.B.; Thelen, K. Cytochrome P450-Mediated Metabolism in the Human Gut Wall. *J. Pharm. Pharmacol.* **2009**, *61*, 541–558. [CrossRef] [PubMed]
47. Canaparo, R.; Finnström, N.; Serpe, L.; Nordmark, A.; Muntoni, E.; Eandi, M.; Rane, A.; Zara, G.P. Expression of CYP3A Isoforms and P-Glycoprotein in Human Stomach, Jejunum and Ileum. *Clin. Exp. Pharmacol. Physiol.* **2007**, *34*, 1138–1144. [CrossRef]
48. Srinivas, M. Cytochrome P450 Enzymes, Drug Transporters and Their Role in Pharmacokinetic Drug-Drug Interactions of Xenobiotics: A Comprehensive Review. *Open J. Chem.* **2017**, 001–011. [CrossRef]
49. Heleno, S.A.; Martins, A.; Queiroz, M.J.R.P.; Ferreira, I.C.F.R. Bioactivity of Phenolic Acids: Metabolites versus Parent Compounds: A Review. *Food Chem.* **2015**, *173*, 501–513. [CrossRef] [PubMed]
50. Karhunen, T.; Tilgmann, C.; Ulmanen, I.; Julkunen, I.; Panula, P. Distribution of Catechol-O-Methyltransferase Enzyme in Rat Tissues. *J. Histochem. Cytochem.* **1994**, *42*, 1079–1090.
51. Meech, R.; Mackenzie, P.I. Structure and Function of Uridine Diphosphate Glucuronosyltransferases. *Clin. Exp. Pharmacol. Physiol.* **1997**, *24*, 907–915. [CrossRef]
52. Moroy, G.; Martiny, V.Y.; Vayer, P.; Villoutreix, B.O.; Miteva, M.A. Toward in Silico Structure-Based ADMET Prediction in Drug Discovery. *Drug Discov. Today* **2012**, *17*, 44–55. [CrossRef]
53. Pereira De Sousa, I.; Bernkop-Schnürch, A. Pre-Systemic Metabolism of Orally Administered Drugs and Strategies to Overcome It. *J. Control. Release* **2014**, *192*, 301–309. [CrossRef]
54. Rowland, A.; Miners, J.O.; Mackenzie, P.I. The UDP-Glucuronosyltransferases: Their Role in Drug Metabolism and Detoxification. *Int. J. Biochem. Cell Biol.* **2013**, *45*, 1121–1132. [CrossRef] [PubMed]
55. Billat, P.-A.; Roger, E.; Faure, S.; Lagarce, F. Models for Drug Absorption from the Small Intestine: Where Are We and Where Are We Going? *Drug Discov. Today* **2017**, *22*, 761–775. [CrossRef]
56. Zhu, L.; Lu, L.; Wang, S.; Wu, J.; Shi, J.; Yan, T.; Xie, C.; Li, Q.; Hu, M.; Liu, Z. Oral Absorption Basics: Pathways and Physicochemical and Biological Factors Affecting Absorption. In *Developing Solid Oral Dosage Forms*; Academic Press: Waltham, MA, USA, 2017; pp. 297–329. ISBN 978-0-12-802447-8.
57. Chmiel, T.; Mieszkowska, A.; Kempińska-Kupczyk, D.; Kot-Wasik, A.; Namieśnik, J.; Mazerska, Z. The Impact of Lipophilicity on Environmental Processes, Drug Delivery and Bioavailability of Food Components. *Microchem. J.* **2019**, *146*, 393–406. [CrossRef]
58. López-Yerena, A.; Perez, M.; Vallverdú-Queralt, A.; Escribano-Ferrer, E. Insights into the Binding of Dietary Phenolic Compounds to Human Serum Albumin and Food-Drug Interactions. *Pharmaceutics* **2020**, *12*, 1123. [CrossRef] [PubMed]

59. Castejón, M.L.; Montoya, T.; Alarcón-de-la-Lastra, C.; Sánchez-Hidalgo, M. Potential Protective Role Exerted by Secoiridoids from Olea Europaea L. in Cancer, Cardiovascular, Neurodegenerative, Aging-Related, and Immunoinflammatory Diseases. *Antioxidants* **2020**, *9*, 149. [CrossRef] [PubMed]
60. Chan, J.M. Drug Metabolism and Pharmacogenetics. In Pharmacology and Physiology for Anesthesia. Elsevier: Amsterdam, The Netherlands, 2019; pp. 70–90. ISBN 978-0-323-48110-6.
61. Yilmaz, Y.; Williams, G.; Walles, M.; Manevski, N.; Krähenbühl, S.; Camenisch, G. Comparison of Rat and Human Pulmonary Metabolism Using Precision-Cut Lung Slices (PCLS). *Drug Metab. Lett.* **2019**, *13*, 53–63. [CrossRef]
62. Fatouros, M.; Bourantas, K.; Bairaktari, E.; Elisaf, M.; Tsolas, O.; Cassioumis, D. Role of the Spleen in Lipid Metabolism. *Br. J. Surg.* **1995**, *82*, 1675–1677. [CrossRef]
63. Miners, J.; Yang, X.; Knights, K.; Zhang, L. The Role of the Kidney in Drug Elimination: Transport, Metabolism, and the Impact of Kidney Disease on Drug Clearance. *Clin. Pharmacol. Ther.* **2017**, *102*, 436–449. [CrossRef] [PubMed]